

Article

Mechanistic Insight into Degradation of Cetirizine under UV/Chlorine Treatment: Experimental and Quantum Chemical Studies

Boyi Zhu [†], Fangyuan Cheng [†], Wenjing Zhong, Jiao Qu, Ya-nan Zhang ^{*} and Hongbin Yu ^{*}

State Environmental Protection Key Laboratory of Wetland Ecology and Vegetation Restoration, School of Environment, Northeast Normal University, Changchun 130117, China; zhuby551@nenu.edu.cn (B.Z.); chengfy310@nenu.edu.cn (F.C.); zhongwj598@nenu.edu.cn (W.Z.); quj100@nenu.edu.cn (J.Q.)

^{*} Correspondence: zhangyn912@nenu.edu.cn (Y.-n.Z.); yuhb108@nenu.edu.cn (H.Y.)

[†] These authors contributed equally to this work.

Abstract: UV/chlorine treatment is an efficient technology for removing organic pollutants in wastewater. Nevertheless, degradation of antihistamines in the UV/chlorine system, especially the underlying reaction mechanism, is not yet clear. In this study, the degradation of cetirizine (CTZ), a representative antihistamine, under UV/chlorine treatment was investigated. The results showed that CTZ could undergo fast degradation in the UV/chlorine system with an observed reaction rate constant (k_{obs}) of $(0.19 \pm 0.01) \text{ min}^{-1}$, which showed a first-increase and then-decrease trend with its initial concentration increased. The degradation of CTZ during the UV/chlorine treatment was attributed to direct UV irradiation (38.7%), HO^\bullet (35.3%), Cl^\bullet (7.3%), and ClO^\bullet (17.1%). The k_{obs} of CTZ decreased with the increase in pH and the increase in concentrations of a representative dissolved organic matter, Suwannee River natural organic matter (SRNOM), due to their negative effects on the concentrations of reactive species generated in the UV/chlorine system. The detailed reaction pathways of HO^\bullet , ClO^\bullet , and Cl^\bullet with CTZ were revealed using quantum chemical calculation. This study provided significant insights into the efficient degradation and the underlying mechanism for the removal of CTZ in the UV/chlorine system.

Keywords: UV/chlorine; cetirizine; reactive species; dissolved organic matter; reaction pathway



Citation: Zhu, B.; Cheng, F.; Zhong, W.; Qu, J.; Zhang, Y.-n.; Yu, H. Mechanistic Insight into Degradation of Cetirizine under UV/Chlorine Treatment: Experimental and Quantum Chemical Studies. *Water* **2022**, *14*, 1323. <https://doi.org/10.3390/w14091323>

Academic Editors: Cassan Hodaif, Antonio Zuorro, Joaquín R. Dominguez, Juan García Rodríguez, José A. Peres and Zacharias Frontistis

Received: 26 March 2022

Accepted: 18 April 2022

Published: 19 April 2022

Publisher's Note: MDPI stays neutral with regard to jurisdictional claims in published maps and institutional affiliations.



Copyright: © 2022 by the authors. Licensee MDPI, Basel, Switzerland. This article is an open access article distributed under the terms and conditions of the Creative Commons Attribution (CC BY) license (<https://creativecommons.org/licenses/by/4.0/>).

1. Introduction

Pharmaceuticals and personal care products (PPCPs) have attracted widespread attention because of their ubiquity in the aqueous environment and potentially high risks to the ecosystem [1–3]. Antihistamines, as one kind of PPCPs, are mainly used to alleviate human allergies [4]. In recent years, antihistamines have been frequently detected in the environment due to the extensive production and widespread use [5]. The concentrations of antihistamines in surface water have been found to be mainly at ng L^{-1} level, and high concentrations up to $\mu\text{g L}^{-1}$ level were also reported [6,7]. The antihistamines in surface water are mainly discharged from wastewater treatment plants (WWTPs), of which effluent contains antihistamines with concentrations as high as mg L^{-1} level [7]. Although antihistamines have been produced and used as specific histamine H1-receptor antagonists, the toxic effects, e.g., cardiotoxicity and sublethal effects, of frequently used antihistamines to aquatic organisms have been observed [6,8,9]. Thus, it is of great significance to remove antihistamines in wastewater before their discharging into natural waters.

Nowadays, the mainly used treatment technologies in WWTPs cannot effectively remove organic pollutants [10,11], especially PPCPs [12,13]. Antihistamines have been also ineffectively or inefficiently degraded by the traditionally used technologies due to their high concentration in the effluent from WWTPs [7,14]. Advanced oxidation processes (AOPs), including ozonation, ultraviolet (UV)/ H_2O_2 , etc., have been proven to be effective

technologies for degrading refractory PPCPs, including antihistamines [5,15,16]. The antihistamines, e.g., cimetidine (CMD), cetirizine (CTZ), and diphenhydramine (DPD), have been shown to undergo degradation in TiO₂-initiated photocatalysis [17], ozonation and peroxymonosulfate oxidation [5,18], and UV/H₂O₂ treatment [19], respectively.

Among various AOPs, UV/chlorine technology is attractive due to its efficient degradation of various pollutants [20–22]. In a UV/chlorine system, reactive species with high reactivity such as hydroxyl radicals (HO•) and chlorine free radicals (including Cl•, ClO•, and Cl₂•⁻) were generated, which dominated the degradation of organic contaminants [23]. For example, Lei et al. [24] found that two representative antihistamines, cimetidine and famotidine, could undergo fast reaction with HO•, Cl•, and Cl₂•⁻, and the reaction rate constants were $6.50 \times 10^9 \text{ M}^{-1} \text{ s}^{-1}$, $1.46 \times 10^{10} \text{ M}^{-1} \text{ s}^{-1}$, and $0.43 \times 10^{10} \text{ M}^{-1} \text{ s}^{-1}$ and $1.72 \times 10^{10} \text{ M}^{-1} \text{ s}^{-1}$, $2.78 \times 10^9 \text{ M}^{-1} \text{ s}^{-1}$, and $1.65 \times 10^9 \text{ M}^{-1} \text{ s}^{-1}$, respectively. Therefore, it can be reasonably speculated that antihistamines can be efficiently degraded in the UV/chlorine process. However, little attention has been paid on the removal of antihistamines. Furthermore, the contribution of these reactive species to the degradation of antihistamines in the UV/chlorine system is also unclear.

The degradation of PPCPs in a UV/chlorine system was reported to be influenced by aqueous environmental factors [25]. For example, pH can affect free chlorine's dissociation and subsequently influence the generation of reactive species [26], and also change the reactivity of ionizable active pharmaceuticals with the generated reactive species during the UV/chlorine process [27]. During the UV/chlorine treatment, dissolved organic matter (DOM), which is a ubiquitous component in wastewater, was shown to inhibit the degradation of two PPCPs (naproxen and gemfibrozil) via inner filter effect and quenching of the generated reactive species [25]. The water matrix could not only influence the degradation efficiency but also affect the degradation pathways of PPCPs by changing the generation and presence of reactive species during the UV/chlorine treatment. The reactivity of the generated reactive species toward PPCPs was shown to be structure-dependent [28].

The reaction of the reactive species in a UV/chlorine system with PPCPs could lead to the formation of toxic by-products [29], and the formation of halogenated intermediates in the reactions of reactive chlorine radicals with PPCPs is a great concern in the use of the UV/chlorine technology [28]. Therefore, it is essential to investigate the detailed reaction pathways of the reactive species such as HO•, Cl•, Cl₂•⁻, and ClO• with PPCPs. The reactions of these reactive species with organic pollutants mainly occur through single electron transfer, abstraction of hydrogen (H-abstraction), and addition pathways [30–32]. Quantum chemical calculation has been previously applied to investigate the reactions of reactive species with organic contaminants successfully [32,33], and the results demonstrated that H-abstraction and addition are the major reaction pathways [21]. Nevertheless, the reaction pathways of antihistamines with the generated reactive species in the UV/chlorine system are still unclear and worthy of urgent research.

Thus, the degradation of antihistamines in a UV/chlorine system was investigated with CTZ as a representative, which is among the most detected antihistamines with the highest concentrations in the effluent and surface water [7]. The effect of pH, initial concentration, and SRNOM (a representative of DOM) on the degradation of CTZ was revealed. Furthermore, the contribution of the reactive species on the degradation of CTZ was investigated, and the detailed reaction pathways of these reactive species with CTZ were calculated using quantum chemical calculation. The results of this study were helpful for providing alternative technology to remove antihistamines in wastewater as well as deep insight into the degradation mechanisms of emerging PPCPs in the UV/chlorine system.

2. Materials and Methods

2.1. Chemicals

CTZ (98%), sodium hypochlorite solution (available chlorine 5%), nitrobenzene (NB, 98%), and tert-butanol (TBA, chromatographical purity) were purchased from J&K Scientific Ltd. (Beijing, China). SRNOM (2R101N) was obtained from the International Humic

Substances Society. Na_2HPO_4 and NaH_2PO_4 were purchased from Tianjin Damao Chemical (Tianjin, China). Methanol (chromatographic purity) was purchased from TEDIA (Fairfield, CT, USA). Ultrapure water was produced using an instrument purchased from Chengdu Ultrapure Technology Co., Ltd. (Chengdu, China).

2.2. UV/Chlorine Degradation Experiments

The experiments were performed in an OCRS-PX32T rotatable photochemical reactor that was obtained from Kaifeng HXsei Science Instrument Factory (Kaifeng, China) (Figure S1). The light source used in this study was a 500 W mercury lamp with main wavelengths of 254 nm and 297 nm, of which light intensity was determined to be $(1.45 \pm 0.07) \text{ mW cm}^{-2}$ and $(0.57 \pm 0.03) \text{ mW cm}^{-2}$ using a UV-B dual-channel ultraviolet radiation meter (Photoelectric Instrument Factory of Beijing Normal University, Beijing, China). During the treatment, the temperature was controlled at $(25 \pm 1) ^\circ\text{C}$ using a circulating cooling water system. All experiments were conducted in triplicate.

The initial concentration of CTZ and free chlorine was $10 \mu\text{M}$ and $100 \mu\text{M}$, respectively (Phosphate buffer solution (PBS), pH 7.0). The UV-Vis absorption spectra of NaClO and CTZ are shown in Figure S2. UV/chlorine treatment was performed in the photo-reactor for 10 min. During the irradiation, dark control experiments were conducted with quartz tubes (30 mL) covered using aluminum foil. Samples were obtained and placed in dark conditions at room temperature during the UV/chlorine treatment. The concentration of residual chlorine was determined with the method that we used in our previous study [34].

The effects of the initial concentration of CTZ (2, 5, 10, 25, and $50 \mu\text{M}$) and free chlorine (100, 200, 500, and $700 \mu\text{M}$) on the degradation of CTZ was investigated by changing the concentrations. SRNOM was added with concentrations of 2.0, 5.0, 10.0, and 15.0 mg L^{-1} to investigate its effect on the degradation of CTZ. NB ($2 \mu\text{M}$) was used as the quencher of HO^\bullet [35], sodium bicarbonate (NaHCO_3 , 100 mM) was used to scavenge the HO^\bullet , Cl^\bullet , and $\text{Cl}_2^{\bullet-}$ [28], and TBA (100 mM) was employed as the quencher of HO^\bullet , Cl^\bullet , and ClO^\bullet [36]. During the degradation of CTZ, Cl^- with high concentration of 50 mM was added to investigate the roles of Cl^\bullet and $\text{Cl}_2^{\bullet-}$ as it can convert Cl^\bullet to $\text{Cl}_2^{\bullet-}$ [27].

2.3. Analytical Methods

An Agilent 1260 II HPLC (Agilent Technologies Inc., Santa Clara, CA, USA) with a diode array detector was used to quantify CTZ. During the quantification, a Welch Ultimate™ AQ-C18 ($250 \text{ mm} \times 4.6 \text{ mm}$, 5 m) analysis column (Welch Materials Inc., Maryland, USA) was used. The mobile phase for the detection of CTZ was methanol and 0.1% phosphoric acid solution aqueous (pH 2.3) with a ratio of 60:40, and the wavelength selected for the detection of CTZ was 200 nm.

2.4. Quantum Chemical Calculation Methods

All quantum chemical calculation was performed with Gaussian 16 software [37]. The optimization and single-point energy calculation were performed using density functional theory (DFT) with the function of B3LYP. The optimization was performed at the level of 6-31+G(d, p), and the single-point energy calculation was performed at the level of 6-311++G(3df, 2p). The integral equation form of the polarization continuum model (IEFPCM) was used to consider the solvent effect of water. The transition state (TS) was obtained and characterized by the virtual vibration frequency (only one), and was verified with intrinsic reaction coordinate (IRC) analysis. The thermodynamic energies, i.e., Gibbs free energy and enthalpy, were obtained and zero-point correction was performed while calculating these energies.

3. Results and Discussion

3.1. Degradation of CTZ and Influencing Factors during UV/Chlorine Treatment

During direct UV irradiation, obvious degradation of CTZ was observed and no obvious degradation in the dark controls was observed (Figure 1). These results indicate

that CTZ was photodegradable under direct UV irradiation, and the degradation of CTZ followed pseudo first-order kinetics. The observed degradation rate constant (k_{obs}) of CTZ under direct UV irradiation was calculated to be $(0.08 \pm 0.01) \text{ min}^{-1}$. In a previous study, the photodegradation of CTZ under UV irradiation was also observed [38]. In the UV/chlorine system, the degradation rate of CTZ was faster than that under direct UV irradiation ($p < 0.05$, Figure 1). The k_{obs} of CTZ increased to (0.19 ± 0.01) , (0.29 ± 0.02) , (0.42 ± 0.03) , and $(0.50 \pm 0.02) \text{ min}^{-1}$ with concentrations of free chlorine increased to 100, 200, 500, and 700 μM , respectively. These results demonstrated the important role of free chlorine in the removal of CTZ. The degradation efficiency reached up to 84.9% within 10 min of treatment and exceeded 90% within 15 min of treatment at the free chlorine concentration of 100 μM in the UV/chlorine system. Thus, the free chlorine concentration of 100 μM was selected in the following experiments.

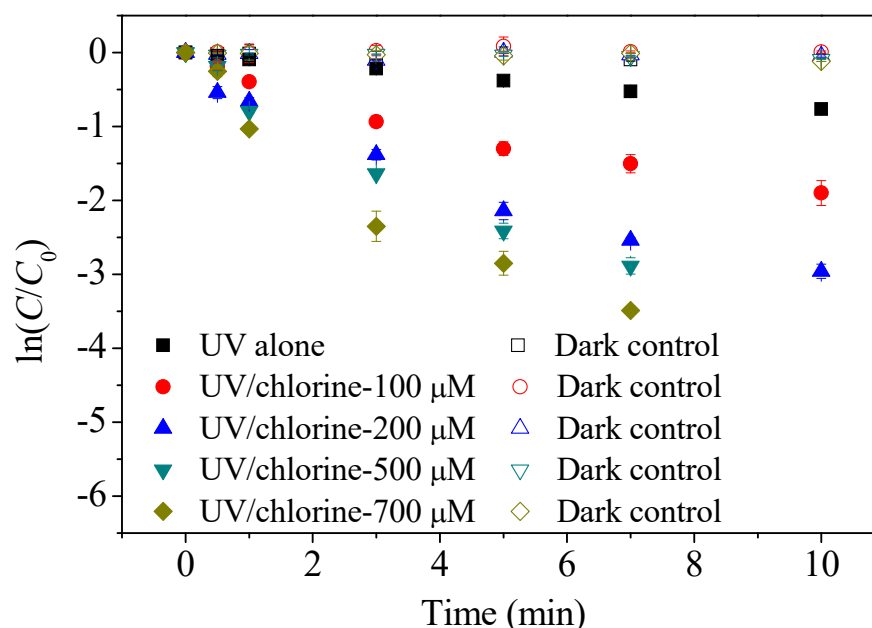


Figure 1. Degradation kinetics of CTZ in UV/chlorine system with different concentration of free chlorine (pH = 7.0, $[\text{CTZ}]_0 = 10 \mu\text{M}$. The error bars represent the 95% confidence interval ($n = 3$)).

In the UV/chlorine system, the initial concentration of organic pollutants was shown to affect their degradation kinetics and efficiencies [39]. Therefore, the effect of initial concentrations of CTZ on its degradation was studied, and the results are exhibited in Figure 2 and Figure S3 in the Supplementary Materials. As shown in Figure 2, the k_{obs} of CTZ showed a first-increase and then-decrease trend under UV irradiation as well as the UV/chlorine treatment. The fastest degradation rate of CTZ was observed with its initial concentration of 10 μM . With the increase in initial concentration of CTZ from 10 μM to 50 μM , the k_{obs} of CTZ under direct UV irradiation and in the UV/chlorine system decreased 36.4% and 64.4%, respectively.

The effect of initial concentration on the degradation of CTZ under direct UV irradiation was attributed to the competitive light absorption effect at the CTZ with high concentrations. The differences in k_{obs} values in the UV/chlorine system compared with those under direct UV irradiation also showed a first-increase and then-decrease trend (Figure 2), indicating that the concentration-dependence in the degradation of CTZ was not only attributed to the UV-induced degradation but also the competing reactions to the generated reactive species.

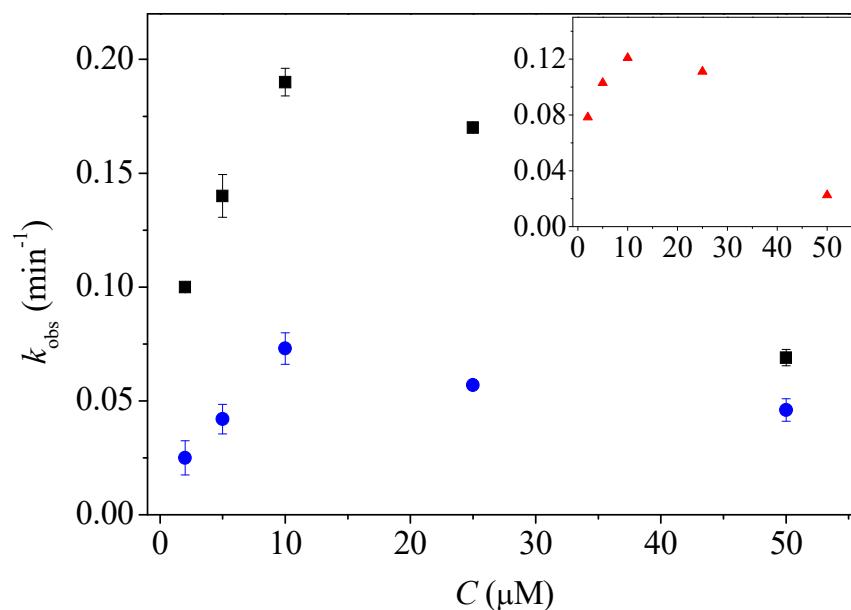


Figure 2. Observed degradation rate constant (k_{obs}) of CTZ with different initial concentration in UV (circle) and UV/chlorine (square) system ($\text{pH} = 7.0$, $(\text{Free chlorine})_0 = 100 \mu\text{M}$). The insert figure represents the differences in k_{obs} values in UV/chlorine system compared with those under UV treatment alone. The error bars represent the 95% confidence interval ($n = 3$).

The influence of pH on the degradation of CTZ was studied and the results showed that the k_{obs} of CTZ decreased with the increase in pH in the UV/chlorine system (Figure 3 and Figure S4 in the Supplementary Materials). There were two possible mechanisms for the pH-dependence of CTZ degradation: (1) the different reactivities of the generated reactive species toward CTZ of different forms, i.e., neutral form and anionic form; (2) the dissociation of HOCl/OCl^- with pK_a of 7.5 [40] led to different concentrations of the generated reactive species [41]. In this case, the former was not suitable as more than 99.7% CTZ ($\text{pK}_a = 3.5$) existed with anionic form in the solutions with pH above 6.0. Thus, in the UV/chlorine system, the decrease in k_{obs} of CTZ with the increase in pH was due to the dissociation of HOCl to OCl^- as the generation quantum yield of reactive species was higher and radical scavenging effect was weaker for HOCl compared with those of OCl^- [42].

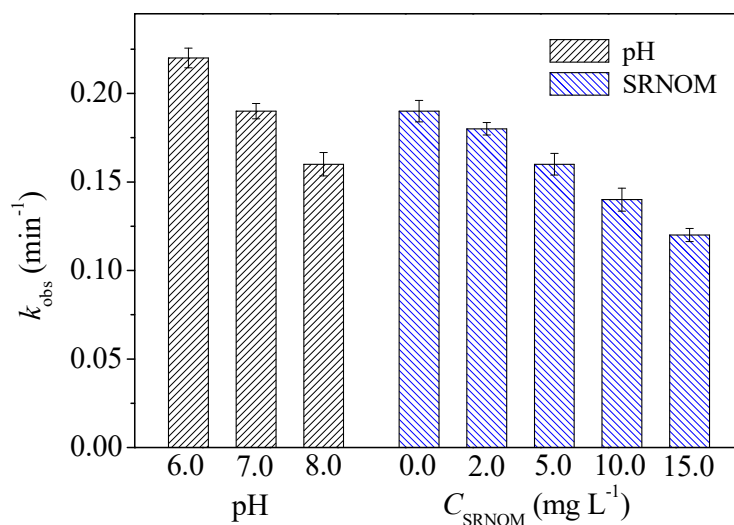


Figure 3. Observed degradation rate constant (k_{obs}) of CTZ in UV/chlorine system in different pH or in the presence of SRNOM with different initial concentrations ($[\text{CTZ}]_0 = 10 \mu\text{M}$, $(\text{Free chlorine})_0 = 100 \mu\text{M}$). The error bars represent the 95% confidence interval ($n = 3$).

The DOM in the wastewater, which was shown to significantly inhibit the removal of primidone and caffeine in the UV/chlorine system, is considered to be a great defect during the practical application of UV/chlorine technology [39]. As exhibited in Figure 3 and Figure S5 in the Supplementary Materials, in the UV/chlorine system, the presence of SRNOM obviously decreased the k_{obs} of CTZ ($p < 0.05$), and the inhibitory effect of SRNOM increased with the increase in its concentration. The k_{obs} of CTZ decreased from $(0.19 \pm 0.01) \text{ min}^{-1}$ without SRNOM to (0.18 ± 0.01) , (0.16 ± 0.01) , (0.14 ± 0.01) , and $(0.12 \pm 0.01) \text{ min}^{-1}$ in the presence of SRNOM with concentrations of 2.0, 5.0, 10.0, and 15.0 mg L^{-1} , respectively, of which decreased rates were 7.3%, 17.8%, 28.4%, and 38.9%, respectively. The inhibition on the degradation of CTZ induced by SRNOM was attributed to: (1) the light screening effect of SRNOM as it can absorb light with wavelengths from 200 to 400 nm (Figure S1); (2) the competition with reactive radicals as reported in a previous study [39]. Thus, it could be concluded that the DOM in wastewater is an unfavorable factor during the degradation of antihistamines in wastewater using UV/chlorine technology.

3.2. Roles of Reactive Species in Degradation of CTZ

In the UV/chlorine system, the underlying degradation mechanisms of CTZ were revealed by performing quenching experiments. As can be seen in Figure 4, the presence of Cl^- significantly decreased the k_{obs} of CTZ in the UV/chlorine system ($p < 0.05$), indicating the involvement of Cl^\bullet in the degradation of CTZ as Cl^- can quench Cl^\bullet to generate $\text{Cl}_2^{\bullet-}$ rapidly [27]. In the presence of NB, the k_{obs} of CTZ decreased to $(0.12 \pm 0.01) \text{ min}^{-1}$ from $(0.19 \pm 0.01) \text{ min}^{-1}$ in the PBS ($p < 0.05$), which indicated the involvement of HO^\bullet during the degradation of CTZ. The presence of HCO_3^- , which could quench HO^\bullet , Cl^\bullet , and $\text{Cl}_2^{\bullet-}$ [28], decreased the k_{obs} of CTZ to $(0.11 \pm 0.01) \text{ min}^{-1}$ ($p < 0.05$). The contribution of Cl^\bullet and $\text{Cl}_2^{\bullet-}$ ($k_{\text{obs}}(\text{NB}) - k_{\text{obs}}(\text{HCO}_3^-)$) was comparable with that of Cl^\bullet ($k_{\text{obs}}(\text{PBS}) - k_{\text{obs}}(\text{Cl}^-)$) in the degradation of CTZ, which demonstrated the negligible effect of $\text{Cl}_2^{\bullet-}$ on the degradation of CTZ. The addition of TBA, which quenches HO^\bullet , Cl^\bullet , and ClO^\bullet [36], further decreased the k_{obs} of CTZ compared with that of HCO_3^- , which indicated the involvement of ClO^\bullet in the degradation of CTZ.

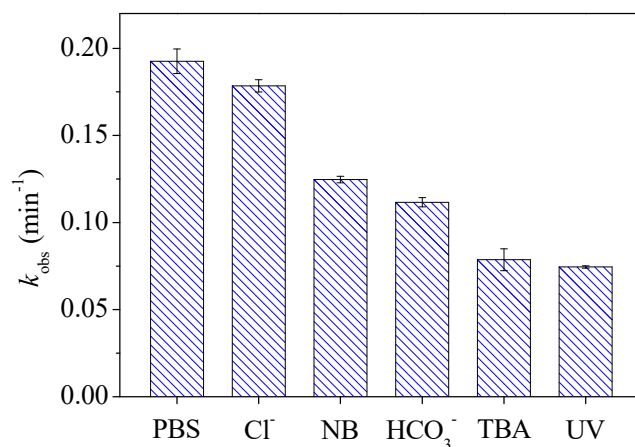


Figure 4. Observed degradation rate constant (k_{obs}) of CTZ ($10 \mu\text{M}$) in UV/chlorine system ((Free chlorine) $_0 = 100 \mu\text{M}$) under different conditions (PBS, pH = 7.0; $\text{Cl}^- = 50 \text{ mM}$; NB (nitrobenzene) = $2 \mu\text{M}$; $\text{HCO}_3^- = 100 \text{ mM}$; TBA (*tert*-butanol) = 100 mM) and in UV system as a control (the error bars represent the 95% confidence interval ($n = 3$)).

In the UV/chlorine system, the presence of SRNOM could inhibit the degradation of CTZ (Figure 3). Thus, the involvement of the reactive species in the degradation of CTZ in SRNOM solutions was also investigated. The addition of the quenchers decreased the k_{obs} of CTZ in the SRNOM solutions (Figure 5), which was similar with those in the PBS. Thus, in the presence of SRNOM, HO^\bullet , Cl^\bullet , and ClO^\bullet were also involved in the degradation of CTZ.

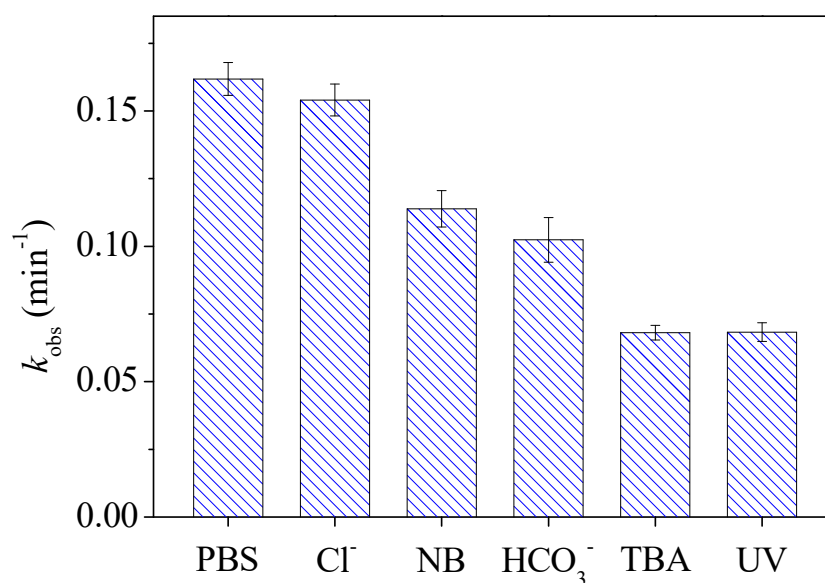


Figure 5. Observed degradation rate constant (k_{obs}) of CTZ (10 μM) in the presence of SRNOM (5 mg L^{-1}) in UV/chlorine system ((Free chlorine)₀ = 100 μM) under different conditions (PBS, pH = 7.0; (Cl^-) = 50 mM; (NB (nitrobenzene)) = 2 μM ; (HCO_3^-) = 100 mM; (TBA (*tert*-butanol)) = 100 mM) and in UV system as a control (the error bars represent the 95% confidence interval ($n = 3$)).

Contribution ratios of the reactive species (HO^\bullet , Cl^\bullet , and ClO^\bullet) and direct UV irradiation to the degradation of CTZ were calculated, and the values are shown in Table S1 in the SI. The contribution ratio of UV-induced degradation of CTZ was 38.7% in the PBS. For the reactive species, the contribution ratio of HO^\bullet , Cl^\bullet , and ClO^\bullet was 35.3%, 7.3%, and 17.1%, respectively. The remaining 1.6% degradation of CTZ was attributed to other reactive species. Among these reactive species, HO^\bullet played a crucial role during the degradation of CTZ. In SRNOM solutions, the contribution ratio of direct UV-induced degradation of CTZ increased to 42.2% compared with that in the PBS. The contribution ratio of HO^\bullet and Cl^\bullet decreased to 29.6% and 4.8%, respectively, compared with the values in the PBS. However, the contribution ratio of ClO^\bullet increased to 21.2% from 17.1%. These results demonstrated the different role of SRNOM on the quenching of these reactive species.

3.3. Degradation Pathways of CTZ in UV/Chlorine System

Considering the complexity of the reactions for CTZ in the UV/chlorine system, the DFT method was used to investigate the degradation pathways of CTZ in the UV/chlorine system. In wastewater, CTZ mainly exists in anionic form as it is with low pK_a of 3.5. Therefore, the reaction pathways of anionic CTZ with the important reactive species (HO^\bullet , Cl^\bullet , and ClO^\bullet) were calculated with DFT methods. As shown in a previous study, major reactions of these reactive species with small organic chemicals are through H-abstraction and addition pathways [21]. For anionic CTZ, there are 24 H-abstraction and 12 addition pathways (Figure 6). All these possible reaction pathways of HO^\bullet , Cl^\bullet , and ClO^\bullet with CTZ were calculated, and the calculated values of Gibbs free energy change (ΔG), activation free energy (ΔG^\ddagger), and enthalpy change (ΔH) for these reaction pathways are listed in Tables S2 and S3. The reaction complexes, transition states, and reaction intermediates of these reactions are shown in Figures S6–S10 in the Supplementary Materials.

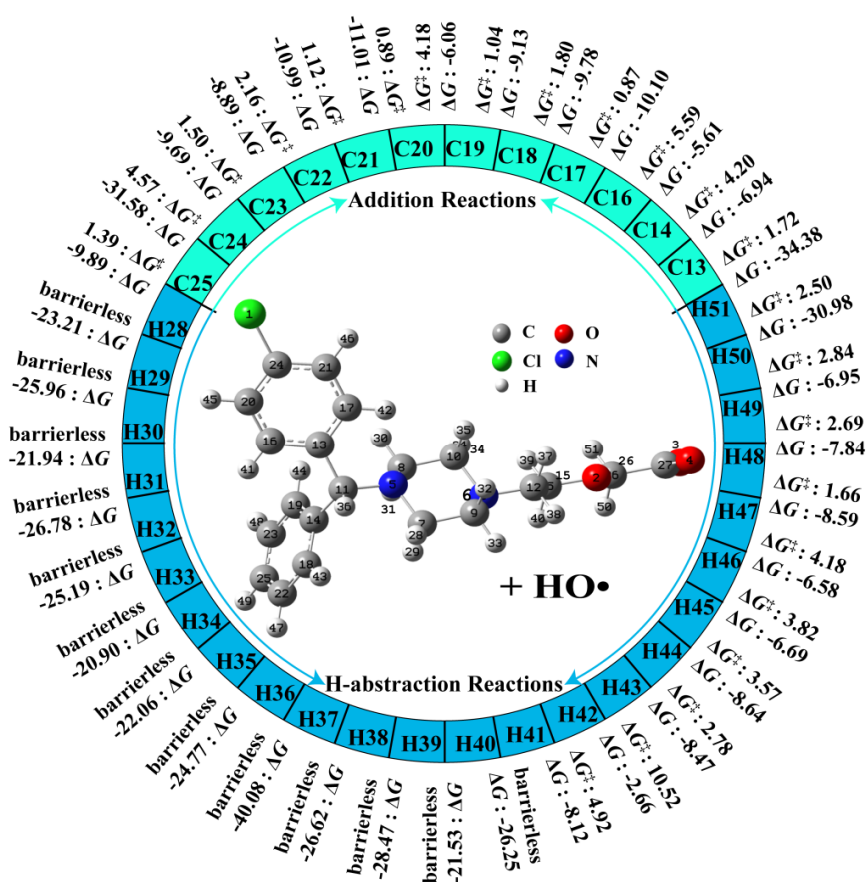


Figure 6. Addition and H-abstraction reaction pathways for reaction of CTZ with HO• (ΔG : Gibbs free energy change; ΔG^\ddagger : activation free energy; unit in kcal mol⁻¹).

For the HO•-initiated H-abstraction and addition reactions, the values of ΔG and ΔH were all < 0 (Figure 6 and Table S2), implying that H-abstraction from CTZ and HO• addition to the unsaturated bonds of the phenyl group of CTZ were all thermodynamically spontaneous. The values of ΔG^\ddagger for the addition reactions were from 0.87 to 5.59 kcal mol⁻¹, indicating that these reactions were also dynamically possible. The HO• additions on the C16 and C20 sites were with low ΔG^\ddagger values (0.87 and 0.89 kcal mol⁻¹, respectively), which indicated that the addition reactions at the two sites were more favorable. For the H-abstraction reactions, the ΔG^\ddagger values for the pathways from the phenyl group (H41–49) and α -carbon (α -C) are from 1.72 to 10.52 kcal mol⁻¹, and the pathways from the hydrocarbon chain (except that from the α -C) were all barrierless, which indicated that the H-abstraction reaction from the hydrocarbon chain of CTZ was more favorable. These results demonstrated the high reactivity of HO• with CTZ, which is in accordance with the extremely high reaction rate constant of HO• with CTZ ($8.94 \times 10^9 \text{ M}^{-1} \text{ s}^{-1}$) [43]. Meanwhile, these results are also in agreement with the experimental results that HO• plays an important role during the degradation of CTZ in the UV/chlorine system.

For the ClO• addition pathways, only the ΔG and ΔH for the reaction at the C24 site were negative (Figure 7 and Table S3), indicating that ClO• addition to the unsaturated bonds at the C24 site was thermodynamically spontaneous and exothermic. Thus, although the ΔG^\ddagger values of the addition reaction at the C24 site (17.21 kcal mol⁻¹) were relatively higher compared with that at other sites, ClO• addition reaction could only occur spontaneously at this site. This was due to the generation of a thermodynamically more stable intermediate with an oxygen atom on C24 instead of Cl. The H-abstraction pathways on the phenyl group of CTZ were all thermodynamically nonspontaneous and endothermic as they were all with positive ΔG and ΔH (Table S3). The abstraction reactions of H39, H40, H50, and H51 at the hydrocarbon chain were thermodynamically spontaneous

and exothermic due to their negative ΔG and ΔH (Figure 7 and Table S3). Among these reactions, the abstraction of H50 and H51 were more favorable due to the lower ΔG^\ddagger values (2.22 and 1.83 kcal mol⁻¹, respectively).

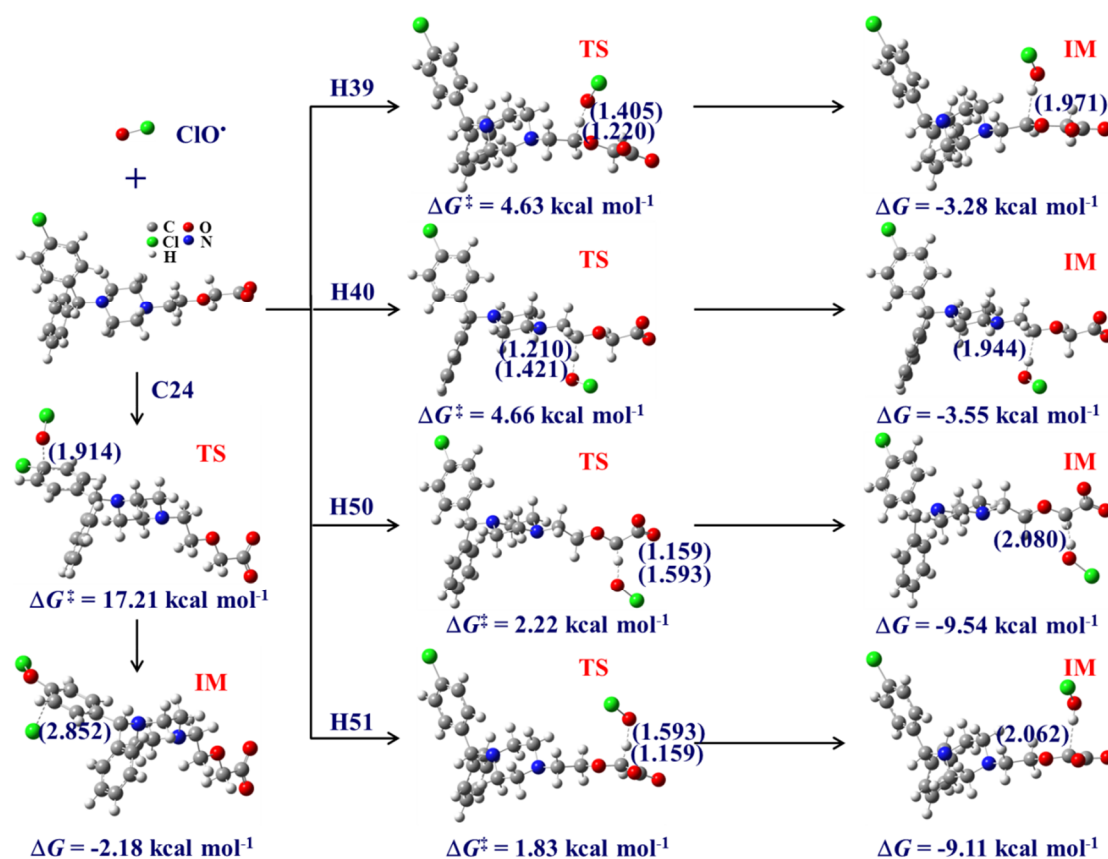


Figure 7. Detailed addition (C24 site) and H-abstraction (H39, H40, H50, and H51) pathways for the reaction of CTZ + ClO• (the values in the brackets are length of bonds marked with the dashed lines, and the unit is Å; TS and IM denote transition state and intermediate, respectively).

For the reaction of CTZ with Cl•, only H-abstraction of H36 was with negative ΔG (−3.08 kcal mol⁻¹), and of which ΔG^\ddagger was 9.54 kcal mol⁻¹, implying that H-abstraction of H36 was thermodynamically spontaneous and dynamically possible. The reaction complex, transition state, and intermediate of this reaction are shown in Figure S11. The results implied that the Cl• showed low reactivity toward CTZ, which is consistent with the experimental results that Cl• played a minor role (7.3%) in the degradation of CTZ in the UV/chlorine system.

For the reactions of CTZ with HO•, Cl•, and ClO•, H-abstraction is the main reaction pathway, which leads to the generation of C-centered radicals. C-centered radicals undergo subsequent reactions with dissolved O₂ or H₂O to form hydroxylated products [30,32]. Addition reaction of HO• and ClO• with CTZ could also lead to the generation of hydroxylated products and the dechlorinated product. Meanwhile, no chlorinated products were generated during the reaction of these reactive species with CTZ. Thus, the degradation of CTZ during the UV/chlorine treatment could decrease the toxicity induced by CTZ.

4. Conclusions

The degradation of an emerging organic pollutant CTZ in the UV/chlorine system was investigated and the underlying reaction mechanism was revealed by combining the methods of experiment and quantum chemical calculation. The results demonstrated that CTZ could be removed efficiently in the UV/chlorine system, of which degradation was initial-concentration dependent. In the UV/chlorine system, besides direct UV-induced

degradation, the generated HO•, Cl•, and ClO• contributed greatly to the degradation of CTZ, among which HO• played a crucial role in the degradation of CTZ. The HO• and ClO• initiated the degradation of CTZ mainly through addition and H-abstraction reactions, and the Cl• could only initiate H-abstraction reaction.

Supplementary Materials: The following supporting information can be downloaded at: <https://www.mdpi.com/article/10.3390/w14091323/s1>, Figure S1: Photochemical reactor system diagram; Figure S2: UV-Vis absorption spectra of NaClO, CTZ, and SRNOM; Figure S3: Degradation kinetics of CTZ with different concentrations in UV/chlorine system; Figure S4: Degradation kinetics of CTZ in UV/chlorine system with different pH values; Figure S5: Degradation kinetics of CTZ in UV/chlorine system in the presence of SRNOM with different concentration; Figure S6: Reaction complexes, transition states and intermediates of the addition reaction pathways of CTZ with HO•; Figure S7: Reaction intermediates of barrierless H-abstraction reaction pathways of CTZ with HO•; Figure S8: Reaction complexes, transition states and intermediates of the hydrogen abstraction pathways of CTZ with HO•; Figure S9: Reaction complexes, transition states and intermediates of the addition reaction pathways of CTZ with ClO•; Figure S10: Reaction complexes, transition states and intermediates of the hydrogen abstraction reaction pathways of CTZ with ClO•; Figure S11: Reaction complexes, transition states and intermediates of the hydrogen abstraction reaction of H36 of CTZ with Cl•; Table S1: Contribution ratio of different reactive species and UV degradation to the degradation of CTZ in UV/chlorine system; Table S2: Calculated Gibbs free energy change (ΔG), enthalpy change (ΔH) and activation free energy (ΔG^\ddagger) values for possible reaction pathways of HO• with CTZ; Table S3: Calculated Gibbs free energy change (ΔG), enthalpy change (ΔH) and activation free energy (ΔG^\ddagger) values for possible reaction pathways of ClO• with CTZ (in kcal mol⁻¹).

Author Contributions: Conceptualization, Y.-n.Z. and H.Y.; methodology, B.Z. and F.C.; software, B.Z. and F.C.; validation, B.Z., F.C. and W.Z.; formal analysis, B.Z.; investigation, B.Z., F.C. and W.Z.; resources, J.Q., Y.-n.Z. and H.Y.; data curation, B.Z. and F.C.; writing—original draft B.Z.; writing—review and editing, Y.-n.Z. and H.Y.; supervision, Y.-n.Z. and H.Y.; funding acquisition, J.Q., Y.-n.Z. and H.Y. All authors have read and agreed to the published version of the manuscript.

Funding: This research was funded by the National Natural Science Foundation of China, grant number 22176030, 42130705, and 21976027; the Fundamental Research Funds for the Central Universities, grant number 2412019FZ019 and 2412020FZ015, and the Jilin Province Science and Technology Development Projects, grant number 20210101110JC.

Acknowledgments: This work was supported by the National Natural Science Foundation of China (22176030, 42130705, and 21976027), the Fundamental Research Funds for the Central Universities (2412019FZ019 and 2412020FZ015), and the Jilin Province Science and Technology Development Projects (20210101110JC).

Conflicts of Interest: The authors declare no conflict of interest.

References

1. Cheng, Y.-X.; Chen, J.; Wu, D.; Liu, Y.-S.; Yang, Y.-Q.; He, L.-X.; Ye, P.; Zhao, J.-L.; Liu, S.-S.; Yang, B.; et al. Highly enhanced biodegradation of pharmaceutical and personal care products in a novel tidal flow constructed wetland with baffle and plants. *Water Res.* **2021**, *193*, 116870. [[CrossRef](#)] [[PubMed](#)]
2. Ren, B.; Shi, X.; Jin, X.; Wang, X.C.; Jin, P. Comprehensive evaluation of pharmaceuticals and personal care products (PPCPs) in urban sewers: Degradation, intermediate products and environmental risk. *Chem. Eng. J.* **2021**, *404*, 127024. [[CrossRef](#)]
3. Zhang, R.; Meng, T.; Huang, C.-H.; Ben, W.; Yao, H.; Liu, R.; Sun, P. PPCP degradation by chlorine–UV processes in ammoniacal water: New reaction insights, kinetic modeling, and DBP formation. *Environ. Sci. Technol.* **2018**, *52*, 7833–7841. [[CrossRef](#)]
4. Jonsson, M.; Fick, J.; Klaminder, J.; Brodin, T. Antihistamines and aquatic insects: Bioconcentration and impacts on behavior in damselfly larvae (Zygoptera). *Sci. Total Environ.* **2014**, *472*, 108–111. [[CrossRef](#)] [[PubMed](#)]
5. He, X.; O’Shea, K.E. Rapid transformation of H1-antihistamines cetirizine (CET) and diphenhydramine (DPH) by direct peroxy-monosulfate (PMS) oxidation. *J. Hazard. Mater.* **2020**, *398*, 123219. [[CrossRef](#)]
6. Jonsson, M.; Andersson, M.; Fick, J.; Brodin, T.; Klaminder, J.; Piovano, S. High-speed imaging reveals how antihistamine exposure affects escape behaviours in aquatic insect prey. *Sci. Total Environ.* **2019**, *648*, 1257–1262. [[CrossRef](#)]
7. Kristofco, L.A.; Brooks, B.W. Global scanning of antihistamines in the environment: Analyses of occurrence and hazards in aquatic systems. *Sci. Total Environ.* **2017**, *592*, 477–487. [[CrossRef](#)]

8. Bittner, L.; Teixidó, E.; Keddi, I.; Escher, B.I.; Klüvera, N. pH-Dependent uptake and sublethal effects of antihistamines in Zebrafish (*Danio rerio*) embryos. *Environ. Toxicol. Chem.* **2019**, *38*, 1012–1022. [[CrossRef](#)]
9. Paakkari, I. Cardiotoxicity of new antihistamines and cisapride. *Toxicol. Lett.* **2002**, *127*, 279–284. [[CrossRef](#)]
10. Zuorro, A.; Maffei, G.; Lavecchia, R. Kinetic modeling of azo dye adsorption on non-living cells of *Nannochloropsis oceanica*. *J. Environ. Chem. Eng.* **2017**, *5*, 4121–4127. [[CrossRef](#)]
11. Montanaro, D.; Lavecchia, R.; Petrucci, E.; Zuorro, A. UV-assisted electrochemical degradation of coumarin on boron-doped diamond electrodes. *Chem. Eng. J.* **2017**, *323*, 512–519. [[CrossRef](#)]
12. Mar-Ortiz, A.F.; Salazar-Rábago, J.J.; Sánchez-Polo, M.; Rozalen, M.; Cerino-Córdova, F.J.; Loredó-Cancino, M. Photodegradation of antihistamine chlorpheniramine using a novel iron-incorporated carbon material and solar radiation. *Environ. Sci. Water Res. Technol.* **2020**, *6*, 2607. [[CrossRef](#)]
13. Ennouri, R.; Lavecchia, R.; Zuorro, A.; Elaoud, S.C.; Petrucci, E. Degradation of chloramphenicol in water by oxidation on a boron-doped diamond electrode under UV irradiation. *J. Water Process Eng.* **2021**, *41*, 101995. [[CrossRef](#)]
14. Chen, W.-H.; Huang, J.-R.; Lin, C.-H.; Huang, C.-P. Catalytic degradation of chlorpheniramine over GO-Fe₃O₄ in the presence of H₂O₂ in water: The synergistic effect of adsorption. *Sci. Total Environ.* **2020**, *736*, 139468. [[CrossRef](#)]
15. Sun, P.; Meng, T.; Wang, Z.; Zhang, R.; Yao, H.; Yang, Y.; Zhao, L. Degradation of organic micropollutants in UV/NH₂Cl advanced oxidation process. *Environ. Sci. Technol.* **2019**, *53*, 9024–9033. [[CrossRef](#)] [[PubMed](#)]
16. Yang, X.; Sun, J.; Fu, W.; Shang, C.; Li, Y.; Chen, Y.; Gan, W.; Fang, J. PPCP degradation by UV/chlorine treatment and its impact on DBP formation potential in real waters. *Water Res.* **2016**, *98*, 309–318. [[CrossRef](#)] [[PubMed](#)]
17. Park, Y.-K.; Ha, H.-H.; Yu, Y.H.; Kim, B.-J.; Bang, H.-J.; Lee, H.; Jung, S.-C. The photocatalytic destruction of cimetidine using microwave-assisted TiO₂ photocatalysts hybrid system. *J. Hazard. Mater.* **2020**, *391*, 122568. [[CrossRef](#)]
18. Borowska, E.; Bourgin, M.; Hollender, J.; Kienle, C.; McArdell, C.S.; von Gunten, U.D. Oxidation of cetirizine, fexofenadine and hydrochlorothiazide during ozonation: Kinetics and formation of transformation products. *Water Res.* **2019**, *94*, 350–362. [[CrossRef](#)]
19. Yuan, F.; Hu, C.; Hu, X.; Qu, J.; Yang, M. Degradation of selected pharmaceuticals in aqueous solution with UV and UV/H₂O₂. *Water Res.* **2009**, *43*, 1766–1774. [[CrossRef](#)]
20. Guo, K.; Wu, Z.; Yan, S.; Yao, B.; Song, W.; Hua, Z.; Zhang, X.; Kong, X.; Li, X.; Fang, J. Comparison of the UV/chlorine and UV/H₂O₂ processes in the degradation of PPCPs in simulated drinking water and wastewater: Kinetics, radical mechanism and energy requirements. *Water Res.* **2018**, *147*, 184–194. [[CrossRef](#)]
21. Minakata, D.; Kamath, D.; Maetzold, S. Mechanistic insight into the reactivity of chlorine-derived radicals in the aqueous-phase UV–chlorine advanced oxidation process: Quantum mechanical calculations. *Environ. Sci. Technol.* **2017**, *51*, 6918–6926. [[CrossRef](#)] [[PubMed](#)]
22. Yin, K.; Li, T.; Zhang, T.; Zhang, Y.; Yang, C.; Luo, S. Degradation of organic filter 2-Phenylbenzimidazole-5-Sulfonic acid by light-driven free chlorine process: Reactive species and mechanisms. *Chem. Eng. J.* **2022**, *430*, 132684. [[CrossRef](#)]
23. Wu, Z.; Fang, J.; Xiang, Y.; Shang, C.; Li, X.; Meng, F.; Yang, X. Roles of reactive chlorine species in trimethoprim degradation in the UV/chlorine process: Kinetics and transformation pathways. *Water Res.* **2016**, *104*, 272–282. [[CrossRef](#)] [[PubMed](#)]
24. Lei, Y.; Cheng, S.; Luo, N.; Yang, X.; An, T. Rate constants and mechanisms of the reactions of Cl[•] and Cl₂^{•-} with trace organic contaminants. *Environ. Sci. Technol.* **2019**, *53*, 11170–11182. [[CrossRef](#)] [[PubMed](#)]
25. Liu, H.; Hou, Z.; Li, Y.; Lei, Y.; Xu, Z.; Gu, J.; Tian, S. Modeling degradation kinetics of gemfibrozil and naproxen in the UV/chlorine system: Roles of reactive species and effects of water matrix. *Water Res.* **2021**, *202*, 117445. [[CrossRef](#)] [[PubMed](#)]
26. Remual, C.K.; Manley, D. Emerging investigators series: The efficacy of chlorine photolysis as an advanced oxidation process for drinking water treatment. *Environ. Sci. Water Res. Technol.* **2016**, *2*, 565–579. [[CrossRef](#)]
27. Wang, W.L.; Wu, Q.Y.; Huang, N.; Wang, T.; Hu, H.Y. Synergistic effect between UV and chlorine (UV/chlorine) on the degradation of carbamazepine: Influence factors and radical species. *Water Res.* **2016**, *98*, 190–198. [[CrossRef](#)]
28. Guo, K.; Wu, Z.; Shang, C.; Yao, B.; Hou, S.; Yang, X.; Song, W.; Fang, J. Radical chemistry and structural relationships of PPCP degradation by UV/chlorine treatment in simulated drinking water. *Environ. Sci. Technol.* **2017**, *51*, 10431–10439. [[CrossRef](#)]
29. Pan, Y.; Cheng, S.; Yang, X.; Ren, J.; Fang, J.; Shang, C.; Song, W.; Lian, L.; Zhang, X. UV/chlorine treatment of carbamazepine: Transformation products and their formation kinetics. *Water Res.* **2017**, *116*, 254–265. [[CrossRef](#)]
30. Li, M.; Mei, Q.; Han, D.; Wei, B.; An, Z.; Cao, H.; Xie, J.; He, M. The roles of HO[•], ClO[•] and BrO[•] radicals in caffeine degradation: A theoretical study. *Sci. Total Environ.* **2021**, *768*, 144733. [[CrossRef](#)]
31. Ren, X.; Sun, Y.; Fu, X.; Zhu, L.; Cui, Z. DFT comparison of the OH-initiated degradation mechanisms for five chlorophenoxy herbicides. *J. Mol. Modeling* **2013**, *19*, 2249–2263. [[CrossRef](#)]
32. Zhang, Y.; Wang, J.; Chen, J.; Zhou, C.; Xie, Q. Phototransformation of 2,3-dibromopropyl-2,4,6-tribromophenyl ether (DPTE) in natural waters: Important roles of dissolved organic matter and chloride ion. *Environ. Sci. Technol.* **2018**, *52*, 10490–10499. [[CrossRef](#)] [[PubMed](#)]
33. Li, C.; Xie, H.-B.; Chen, J.; Yang, X.; Zhang, Y.; Qiao, X. Predicting gaseous reaction rates of short chain chlorinated paraffins with •OH: Overcoming the difficulty in experimental determination. *Environ. Sci. Technol.* **2014**, *48*, 13808–13816. [[CrossRef](#)] [[PubMed](#)]
34. Zhou, Y.; Cheng, F.; He, D.; Zhang, Y.; Qu, J.; Yang, X.; Chen, J.; Peijnenburg, W.J.G.M. Effect of UV/chlorine treatment on photophysical and photochemical properties of dissolved organic matter. *Water Res.* **2021**, *192*, 116857. [[CrossRef](#)]

35. Wang, J.; Wang, K.; Guo, Y.; Ye, Z.; Guo, Z.; Lei, Y.; Yang, X.; Zhang, L.; Niu, J. Dichlorine radicals ($\text{Cl}_2^{\bullet-}$) promote the photodegradation of propranolol in estuarine and coastal waters. *J. Hazard. Mater.* **2021**, *414*, 125536. [[CrossRef](#)] [[PubMed](#)]
36. Yang, T.; Mai, J.; Wu, S.; Liu, C.; Tang, L.; Mo, Z.; Zhang, M.; Guo, L.; Liu, M.; Ma, J. UV/chlorine process for degradation of benzothiazole and benzotriazole in water: Efficiency, mechanism and toxicity evaluation. *Sci. Total Environ.* **2021**, *760*, 144304. [[CrossRef](#)]
37. Frisch, M.J.; Trucks, G.W.; Schlegel, H.B.; Scuseria, G.E.; Robb, M.A.; Cheeseman, J.R.; Scalmani, G.; Barone, V.; Petersson, G.A.; Nakatsuji, H.; et al. *Gaussian 16, B.01*; Gaussian Inc.: Wallingford, CT, USA, 2016.
38. Gadipelly, C.R.; Rathod, V.K.; Marathe, K.V. Persulfate assisted photo-catalytic abatement of cetirizine hydrochloride from aqueous waste: Biodegradability and toxicity analysis. *J. Mol. Catal. A Chem.* **2016**, *414*, 116–121. [[CrossRef](#)]
39. Wang, Y.; dos Santos, M.M.; Ding, X.; Labanowski, J.; Gombert, B.; Snyder, S.A.; Croué, J.-P. Impact of EfOM in the elimination of PPCPs by UV/chlorine: Radical chemistry and toxicity bioassays. *Water Res.* **2021**, *204*, 117634. [[CrossRef](#)] [[PubMed](#)]
40. Dodd, M.C.; Huang, C. Aqueous chlorination of the antibacterial agent trimethoprim: Reaction kinetics and pathways. *Water Res.* **2007**, *41*, 647–655. [[CrossRef](#)]
41. Fang, J.; Fu, Y.; Shang, C. The roles of reactive species in micropollutant degradation in the UV/free chlorine system. *Environ. Sci. Technol.* **2014**, *48*, 1859–1868. [[CrossRef](#)]
42. Xiang, Y.; Fang, J.; Shang, C. Kinetics and pathways of ibuprofen degradation by the UV/chlorine advanced oxidation process. *Water Res.* **2016**, *90*, 301–308. [[CrossRef](#)] [[PubMed](#)]
43. Cui, D.; DeCaprio, A.; Tarifa, A.; O'Shea, K. Ultrasound-induced remediation of the second-generation antihistamine, Cetirizine. *J. Environ. Chem. Eng.* **2020**, *8*, 103680. [[CrossRef](#)]